An RNA-sequencing study identifies candidate genes for angiotensin II-induced cardiac remodeling

JIN SHU[1*], ZHANWEN LIU[2*], LI JIN[1] and HAIYA WANG[3]

Departments of [1]Gerontology and [2]Pharmacy, Tongren Hospital, Shanghai Jiao Tong University School of Medicine, Shanghai 200336; [3]Department of Gerontology, Renji Hospital Affiliated to Shanghai Jiao Tong University School of Medicine, Shanghai 200001, P.R. China

Received March 13, 2017; Accepted August 24, 2017

DOI: 10.3892/mmr.2017.8043

Abstract. The present study aimed to reveal the underlying mechanism of angiotensin II (AngII)-induced cardiac remodeling and to identify potential therapeutic targets for prevention. Rat cardiac fibroblasts (CFs) were cultured with 10 nM AngII for 12 h, and CFs without AngII were used as the control. Following RNA isolation from AngII treated and control CFs, RNA-sequencing was performed to detect gene expression levels. Differentially-expressed genes (DEGs) were identified using the linear models for microarray analysis package in R software, and their functions and pathways were examined via enrichment analysis. In addition, potential associations at the protein level were revealed via the construction of a protein-protein interaction (PPI) network. The expression levels of genes of interest were validated via reverse transcription-quantitative polymerase chain reaction analysis. In total, 126 upregulated and 140 downregulated DEGs were identified. According to the enrichment analysis, acetyl coA carboxylase β (*ACACB*), interleukin 1β (*IL1B*), interleukin 1α (*IL1A*), nitric oxide synthase 2 (*NOS2*) and matrix metallopeptidase 3 (*MMP3*) were associated with the immune response, regulation of angiogenesis, superoxide metabolic process and carboxylic acid binding biological processes. Among them, *ACACB* and *MPP3* were two predominant nodes in the PPI network. In addition, *IL1B* and *MMP3* were demonstrated to be upregulated. These five genes, particularly *IL1B* and *MMP3*, may be used as candidate markers for the prevention of AngII-induced cardiac remodeling.

Correspondence to: Dr Haiya Wang, Department of Gerontology, Renji Hospital Affiliated to Shanghai Jiao Tong University School of Medicine, 145 Mid Shandong Road, Huangpu, Shanghai 200001, P.R. China
E-mail: haiyawang17@hotmail.com

Mr. Li Jin, Department of Gerontology, Tongren Hospital, Shanghai Jiao Tong University School of Medicine, 1111 Xianxia Road, Shanghai 200336, P.R. China
E-mail: jinli923@126.com

*Contributed equally

Key words: cardiac remodeling, cardiac fibroblasts, angiotensin II, RNA-sequencing, differentially-expressed genes, protein-protein interaction

Introduction

Cardiac remodeling exerts an important role in the development of various cardiovascular diseases, including myocardial infarction and dilated cardiomyopathy. At the initial stage, cardiac remodeling is an adaptive response to external stimuli which maintains normal cardiac function. However, it may become maladaptive and progress into severe decompensation (1). A number of regulators have been reported to be associated with cardiac remodeling, including cytokines and growth factors. For example, transforming growth factor (TGF)-β signaling inhibits the expression of inflammatory cytokines and chemokines by disabling macrophages and promoting the differentiation of myofibroblasts in myocardial infarction and cardiac remodeling (2). Granulocyte colony-stimulating factor has a preventative effect on cardiac dysfunction and remodeling (3).

It has been established that the renin-angiotensin system (RAS) is an important factor that promotes the progression of cardiac remodeling. The effector hormone of RAS, angiotensin II (AngII), has been observed to induce the expression of fibroblast genes and to promote fibroblast proliferation via interactions with the AngII type 1 receptor (4). Therefore, AngII may contribute to cardiac remodeling and is frequently used to induce cardiac remodeling for *in vitro* experiments or in rat model systems (5,6). Although the role of AngII in cardiac remodeling has been established, the downstream factors that affect its function remain to be elucidated. It has been reported that xin actin binding repeat containing 2, a target gene of myocyte-specific enhancer factor 2A, has been demonstrated to be an important regulator in the AngII signaling pathway (7). In addition, platelet-derived growth factor is considered to serve as a downstream factor of AngII and has been proposed as an important regulator of atrial fibrosis (8). However, additional downstream regulators are yet to be identified.

In the present study, an RNA-sequencing (RNA-seq) method was applied to identify differentially-expressed genes (DEGs) in AngII-treated rat cardiac fibroblasts (CFs), compared with those without treatment with AngII. Enrichment analysis was performed to reveal the potential functions and pathways of these important DEGs, and their potential interactions were examined via protein-protein interaction (PPI) network analysis. The expression of genes of interest was validated by reverse transcription-quantitative polymerase chain reaction (RT-qPCR) analysis. Via these comprehensive bioinformatics analyses and gene expression validation experiments, the present study aimed to elucidate the underlying mechanism of AngII-induced cardiac remodeling and to identify potential therapeutic targets for its prevention.

Materials and methods

Cell culture. Rat CFs were purchased from the Type Culture Collection of the Chinese Academy of Sciences (Shanghai, China). Primary rat CFs (n=2) at 50% confluence were cultured in a 12-well plate supplemented with 10 nM AngII for 12 h (AngII group), while those without AngII treatment were used as controls (control group; n=2). Following 12 h of culture, samples in the two groups were harvested for RNA-seq.

RNA isolation and sequencing. Total RNA from each sample was isolated using an RNAiso Plus kit (Takara Biotechnology Co., Ltd., Dalian, China) using the phenol/chloroform extraction method (9). Following dilution, the RNA purity was determined using a NanoDrop 2000 (Thermo Fisher Scientific, Inc., Wilmington, DE, USA). The total RNA (3 μg/sample) was reverse-transcribed to construct a cDNA library, using a NEBNext® Ultra™ RNA Library Prep kit for Illumina® (cat no. E7530L; New England BioLabs, Inc., Ipswich, MA, USA), according to the manufacturer's protocol. The mRNAs were enriched on a magnetic bead, and subsequently sheared into fragments. The random primers, buffer, dNTPs RNase H and DNA polymerase I were added to generate the cDNA. The cDNA was blunt-ended and a single 3' adenosine moiety and Illumina adapters were added to the repaired ends. The cDNAs were amplified via 20 cycles of repair chain reaction, and the thermocycling conditions was as follows: 94˚C for 2 min, 94˚C for 30 sec, then subjected to 5 cycles at 94˚C for 5 sec, 70˚C for 4 min, and subjected to another 5 cycles of 94˚C for 5 sec, 72˚C for 4 min, then 20 cycles of 94˚C for 5 sec, 68˚C for 4 min and a final extension at 70˚C for 10 min. The cDNA clusters were sequenced using the Illumina Hiseq 4000 platform (Illumina, Inc., San Diego, CA, USA) using the 150 paired end method (10). The RNA-seq data was uploaded to the Sequence Read Archive (www.ncbi.nlm.nih.gov/sra) with the accession no. SRP082129.

Pretreatment of RNA-seq data. Quality control of the raw reads was implemented using the prinseq-lite (sourceforge .net/projects/prinseq/files/standalone/) and fastx_toolkit (hannonlab.cshl.edu/fastx_toolkit/index.html) tools as follows: i) Removal of barcode sequences and adaptors of the reads; ii) filtering out of reads with an N content >5%; iii) elimination of the base at each end with a quality <10; iv) exclusion of low-quality reads in which bases with Q<20 accounted for >20% of the length; and v) exclusion of reads with a length <30. Clean reads from the four samples were obtained and aligned with the rat reference genome using TopHat software (version 2.0.8; ccb .jhu.edu/software/tophat/index.shtml) with the default parameters. StringTie (version 1.2.2; ccb.jhu.edu/software/stringtie), a computational method which is able to improve the reconstruction of a transcriptome from RNA-seq reads (11), was utilized to obtain gene annotation information for the aligned raw reads, based on Ensembl (www.ensembl.org).

Identification of DEGs and enrichment analysis. Following pretreatment of the raw RNA-seq data, gene expression levels were obtained by calculating the fragments per kilobase of exon per million fragments mapped (FPKM), using the Cufflinks software (2.2.1 released, cufflinks. cbcb.umd.edu/index.html). Subsequently, the linear models for microarray analysis (limma; www.bioconductor. org/packages/release/bioc/html/limma.html) package in R (www.r-project.org) was used to select DEGs between the treatment and control groups. The thresholds for DEG selection were $|\log_2$ fold change (FC)$|>1$ and $P<0.05$.

The gene ontology database (www.geneontology.org) was utilized to conduct functional enrichment analysis to identify potential biological processes of the DEGs, while the Kyoto Encyclopedia of Genes and Genomes database (www.genome .jp/kegg/pathway.html) was used to perform pathway enrichment analysis to reveal the pathways that may involve the DEGs. The function and pathway enrichment analyses were performed using the Database for Annotation, Visualization and Integrated Discovery online tool (david.abcc.Ncifcrf .gov) (12). The cut-off value for significant function and pathway selection was $P<0.05$.

Construction of PPI network. In order to examine the potential interactions of the DEGs at the protein level, the STRING database online tool (string-db.org) was used to establish the PPI network, under the condition of a combined score >0.4 (13). Cytoscape software (version 3.2.0; cytoscape.org) was used to visualize the network. A node in the PPI network represented the protein product of a DEG, and the degree of a node was deemed to be the number of proteins interacting with this specific node.

RT-qPCR analysis. RNA isolation was performed as described above for RNA-seq. RNAs were transcribed to cDNA using the PrimeScript™ RT Master Mix (Takara Biotechnology Co., Ltd.). qPCR was subsequently performed on an ABI fluorescence quantitative PCR machine (Thermo Fisher Scientific, Inc., Waltham, MA, USA) within a 20 μl reaction system: 10 μl SYBR Green PCR Master Mix (Thermo Fisher Scientific, Inc.), 0.4 μl each primer, 2 μl cDNA templates and 7.2 μl RNase-Free dH_2O. PCR conditions were as follows: Denaturation at 95˚C for 10 min; 40 cycles of 95˚C for 15 sec and 60˚C for 60 sec; and melting at 95˚C for 15 sec, 60˚C for 60 sec and 95˚C for 15 sec. The primer sequences are listed in Table I. β-actin was used as an internal reference gene. The relative expression of each gene was measured using the $2^{-\Delta\Delta Cq}$ method (14).

Statistical analysis. Data are presented as the mean ± standard error of the mean. A Student's t-test using SPSS software

Table I. Primers of validated genes.

Gene	Sequences
β-actin	F: 3'-CCCATCTATGAGGGTTACGC-5'
	R: 3'-TTTAATGTCACGCGATTTC-5'
IL1B	F: 3'-AGCAGCTTTCGACAGTGAGG-5'
	R: 3'-CACACACTAGCAGGTCGTCA-5'
NOS2	F: 3'-TGCTATTCCCAGCCCAACAA-5'
	R: 3'-GAATTCAATGGCTTGAGGCA-5'
DYRK3	F: 3'-CAAGTGCCCACCCTATACAA-5'
	R: 3'-CAGTTGCTCCACCTTCATCAC-5'
MMP3	F: 3'-TTCCTTGGGCTGAAGATGAC-5'
	R: 3'-TCCTGGAGAATGTGAGTGGG-5'
BOLL	F: 3'-CCTGCTTCTTCTGCTCCATTC-5'
	R: 3'-GGCACTTGAAGCATAAACCTG-5'
TNNC2	F: 3'- AGGATGCTAGGGCAGACAC-5'
	R: 3'-TCAAAGATGCGGAAACACTCA-5'
ACACB	F: 3'-CACAAGAAACTGGACCTGC-5'
	R: 3'-CGCGTTCATTACGGAACATC-5'
AXL	F: 3'-AGTGGATTGCTATCGAGAGTCTG-5'
	R:3'-CCTTGACGTAGGTAGTCGTAAATCT-5'

F, forward; R, reverse; IL1B, interleukin 1β; NOS2, nitric oxide synthase 2; DYRK3, dual specificity tyrosine phosphorylation regulated kinase 3; MMP3, matrix metallopeptidase 3; BOLL, boule homolog RNA binding protein; TNNC2, troponin C2 fast skeletal type; ACACB, acetyl coA carboxylase β.

(version 10.0; SPSS, Inc., Chicago, IL, USA) was used to compare the relative expression levels of genes between the two groups. $P<0.05$ was considered to indicate a statistically significant difference. All experiments were repeated three times.

Results

DEGs between AngII treatment group and control group. In the present study, a total of 16,974 genes with FPKM values >0 were detected. Based on the aforementioned criteria, 266 DEGs were selected, including 126 upregulated and 140 downregulated genes. A heat map of the gene expression is presented in Fig. 1, demonstrating that samples in the two groups were able to be distinguished by these DEGs. The top 10 DEGs ranked by FC are presented in Table II, including five upregulated genes [interleukin 1β (*IL1B*), nitric oxide synthase 2 (*NOS2*), dual specificity tyrosine phosphorylation regulated kinase 3 (*DYRK3*), paired box 8 and matrix metallopeptidase 3 (*MMP3*)] and five downregulated genes [boule homolog RNA binding protein (*BOLL*), troponin C2 fast skeletal type (*TNNC2*), F-box protein 2, ankyrin repeat SAM and basic leucine zipper domain containing 1, and MAP6 domain containing 1).

Enrichment analysis of the DEGs. According to the enrichment analysis, the upregulated DEGs were significantly enriched in biological processes (BPs) including response to bacterium [e.g. glutathione peroxidase 2, histone cluster 1 H2B family member 1 (*HIST1H2BL*) and *NOS2*], defense response [e.g., cytochrome b-245 β chain (*CYBB*), *HIST1H2BL* and *NOS2*], immune response (e.g. *CYBB*, linker for activation of T-cells family member 2 and interleukin 20 receptor subunit β), regulation of angiogenesis [e.g. CD36 molecule (*CD36*), C-X3-X motif chemokine ligand 1 and interleukin 1α (*IL1A*)] and superoxide metabolic process (*CYBB*, NADPH oxidase organizer 1 and *NOS2*); and molecular functions (MFs)

Table II. Top ten differentially-expressed genes (ranked by fold-change).

Gene	Log_2 fold change	P-value
IL1B	5.210354306	0.052672383
NOS2	4.874224035	0.000369813
DYRK3	4.454414593	0.001057582
PAX8	4.308293178	0.001274081
MMP3	4.205044062	0.006835961
BOLL	-4.227038973	0.002187013
TNNC2	-4.247495833	0.000384867
FBXO2	-4.285939067	0.003258329
ASZ1	-4.367008762	0.009252033
MAP6D1	-4.397909336	0.018432302

IL1B, interleukin 1β; NOS2, nitric oxide synthase 2; DYRK3, dual specificity tyrosine phosphorylation regulated kinase 3; PAX8, paired box 8; MMP3, matrix metallopeptidase 3; BOLL, boule homolog RNA binding protein; TNNC2, troponin C2 fast skeletal type; FBXO2, F-box protein 2; ASZ1, ankyrin repeat SAM and basic leucine zipper domain containing 1; MAP6D1, MAP6 domain containing 1.

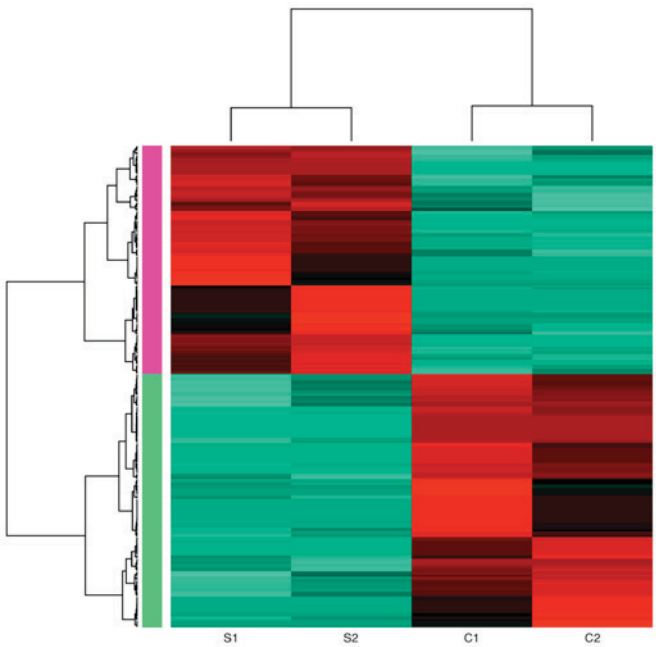

Figure 1. Heat map of the gene expression in angiotensin II-treated samples and controls. X-axis represents samples and Y-axis represents genes. S, sample; C, control.

Table III. Significant enriched functions and pathways for upregulated genes.

Category	Term	Count	Genes	P-value
GOTERM_BP_FAT	GO:0009617~response to bacterium	7	GPX2, HIST1H2BL, BCL3, NOS2, IRG1, IL1A, GCH1	$1.61x10^{-3}$
GOTERM_BP_FAT	GO:0006952~defense response	9	CYBB, IL20RB, HIST1H2BL, BCL3, NOS2, CFI, RT1-BA, IL1A, GCH1	$2.47x10^{-3}$
GOTERM_BP_FAT	GO:0006955~immune response	9	CYBB, LAT2, IL20RB, BCL3, CFI, CX3CL1, RT1-BA, IL1A, GCH1	$3.11x10^{-3}$
GOTERM_BP_FAT	GO:0045765~regulation of angiogenesis	4	CD36, CX3CL1, IL1A, RGD1565355	$5.43x10^{-3}$
GOTERM_BP_FAT	GO:0006801~superoxide metabolic process	3	CYBB, NOXO1, NOS2	$6.82x10^{-3}$
GOTERM_MF_FAT	GO:0031406~carboxylic acid binding	5	CD36, ACACB, NOS2, RGD1565355, GCHFR	$1.82x10^{-2}$
GOTERM_CC_FAT	GO:0005886~plasma membrane	27	CLDN18, CD244, LPPR4, SYT3, CLDN11	$2.57x10^{-3}$
GOTERM_CC_FAT	GO:0044459~plasma membrane part	17	CLDN18, CD244, LPPR4, NOXO1, SLC12A3	$1.05x10^{-2}$
GOTERM_CC_FAT	GO:0009986~cell surface	7	CD244, CD36, LPPR4, CD2, CX3CL1, RT1-BA, IL1A	$2.11x10^{-2}$
GOTERM_CC_FAT	GO:0016021~integral to membrane	36	CD244, CLDN18, LPPR4, GCNT2, SYT3	$4.96x10^{-2}$
KEGG_PATHWAY	rno04670: Leukocyte transendothelial migration	5	CLDN18, CYBB, MYL2, TXK, CLDN11	$1.04x10^{-2}$
KEGG_PATHWAY	rno04514: Cell adhesion molecules	5	NRCAM, CLDN18, CD2, CLDN11, RT1-BA	$2.42x10^{-2}$

Count, number of genes enriched in a specific function or pathway. GO, gene ontology; KEGG, Kyoto Encyclopedia of Genes and Genomes; BP, biological process; CC, cellular component; MF, molecular function.

including carboxylic acid binding [e.g. *CD36*, acetyl coA carboxylase β (*ACACB*) and *NOS2*] (Table III). A total of two significant pathways were enriched, including leukocyte transendothelial migration [e.g. claudin 18 (*CLDN18*), claudin 11 (*CLDN11*) and myosin light chain 2] and cell adhesion molecules (e.g. neuronal cell adhesion molecule, *CLDN18* and *CLDN11*) (Table IV).

The downregulated DEGs were significantly associated with BPs such as visual perception [e.g. γ-aminobutyric acid type A receptor rho2 subunit (*GABRR2*), G protein subunit α transducin 1 (*GNAT1*) and opsin 1 short wave sensitive (*OPN1SW*)], sensory perception of light stimulus (e.g. *GABRR2*, *GNAT1* and *OPN1SW*) and neutral lipid biosynthetic process (e.g. monoacylglycerol O-acyltransferase 1, glycerol-3-phosphate acyltransferase 3 and patatin like phospholipase domain containing 3) and MFs including substrate specific channel activity [e.g. *GABRR2*, potassium voltage-gated channel modifier subfamily S member 1 (*KCNS1*) and potassium two pore domain channel subfamily K member 15 (*KCNK15*)], channel activity (e.g. *GABRR2*, *KCNS1* and *KCNK15*) and passive transmembrane transporter activity (e.g. *GABRR2*, *KCNS1* and *KCNK15*). However, no significant pathway was enriched.

PPI network of the DEGs. Under the criterion of combined score >0.4, a PPI network was established, comprising 112 nodes (representing the protein product of a DEG) and 118 interactions. The top 5 nodes in the PPI network were ACACB (degree=13), GNAT1 (degree=8), MPP3 (degree=7), signal transducer and activator of transcription 4 (degree=6) and myosin-8 (degree=6) (Fig. 2).

Gene expression validations. Reportedly, *AXL*, a novel receptor tyrosine kinase, is closely associated with cardiac remodeling and its expression level is altered by AngII stimulation in vascular smooth muscle cells. Thus, the present study detected its expression levels in CFs by RT-qPCR analysis. The results showed that the expression of *AXL* was downregulated in AngII-treated CFs compared with the control, but this difference was not significant (Fig. 3). In addition, the expression of genes of interest, listed in the top 10 DEGs ranked by FC or top 5 nodes in the PPI network, were detected using RT-qPCR analysis, including *IL1B* (reference no. NM_031512.2), *NOS2* (reference no. NM_012611.3), *DYRK3* (reference no. NM_001024767.1), *MMP3* (reference no. NM_133523.3), *BOLL* (reference no. NM_001113370.1), *ACACB* (reference no. NM_053922.1) and *TNNC2* (reference

Table IV. Significant enriched functions and pathways for downregulated genes.

Category	Term	Count	Genes	P-value
GOTERM_BP_FAT	GO:0007601~visual perception	5	GABRR2, GNAT1, OPN1SW, RGS9, SAG	$2.03x10^{-3}$
GOTERM_BP_FAT	GO:0050953~sensory perception of light stimulus	5	GABRR2, GNAT1, OPN1SW, RGS9, SAG	$2.11x10^{-3}$
GOTERM_BP_FAT	GO:0046460~neutral lipid biosynthetic process	3	MOGAT1, AGPAT9, PNPLA3	$2.69x10^{-3}$
GOTERM_BP_FAT	GO:0046463~acylglycerol biosynthetic process	3	MOGAT1, AGPAT9, PNPLA3	$2.69x10^{-3}$
GOTERM_BP_FAT	GO:0046504~glycerol ether biosynthetic process	3	MOGAT1, AGPAT9, PNPLA3	$3.59x10^{-3}$
GOTERM_MF_FAT	GO:0005216~ion channel activity	9	GABRR2, KCNS1, KCNK15, FXYD4, TRPC5, SLC26A7, CLIC5, KCNIP4, KCNJ13	$6.07x10^{-4}$
GOTERM_MF_FAT	GO:0022838~substrate specific channel activity	9	GABRR2, KCNS1, KCNK15, FXYD4, TRPC5, SLC26A7, CLIC5, KCNIP4, KCNJ13	$7.35x10^{-4}$
GOTERM_MF_FAT	GO:0015267~channel activity	9	GABRR2, KCNS1, KCNK15, FXYD4, TRPC5, SLC26A7, CLIC5, KCNIP4, KCNJ13	$9.35x10^{-4}$
GOTERM_MF_FAT	GO:0022803~passive transmembrane transporter activity	9	GABRR2, KCNS1, KCNK15, FXYD4, TRPC5, SLC26A7, CLIC5, KCNIP4, KCNJ13	$9.35x10^{-4}$
GOTERM_MF_FAT	GO:0005267~potassium channel activity	5	KCNS1, KCNK15, FXYD4, KCNIP4, KCNJ13	$4.78x10^{-3}$
GOTERM_CC_FAT	GO:0000800~lateral element	2	REC8, SYCP3	$4.64x10^{-2}$

Count, number of genes enriched in a specific function or pathway. GO, gene ontology; BP, biological process; CC, cellular component; MF, molecular function.

no. NM_001037351.2). As hypothesized, *IL1B* and *MMP3* were significantly increased under treatment with AngII, compared with the control ($P<0.01$ and $P<0.05$, respectively). However, the expression of other genes did not exhibit any significant alteration between the control and treatment groups ($P>0.05$) (Fig. 3).

Discussion

Adrenergic receptors (ARs) belong to the family of G protein-coupled receptors (GPCRs). Reportedly, ARs are involved in aging and cardiovascular physiopathology (15). In response to stimulation of the sympathetic nervous system, α_1ARs (α_{1A}, α_{1B} and α_{1D}) are able to activate $G\alpha_q$, which contributes to cardiac remodeling (16). AngII is another GPCR that is involved in cardiac remodeling (17). In the present study, AngII was used to treat the rat CFs, and a number of important genes for AngII-induced cardiac remodeling were identified, including *ACACB*, *IL1B*, *IL1A*, *NOS2* and *MMP3*. Among them, *IL1B* and *MMP3* were demonstrated to be upregulated. The majority of the genes were associated with the defense response, immune response, regulation of angiogenesis, superoxide metabolic process and carboxylic acid binding BPs. In addition, ACACB and MPP3 were two of the predominant nodes in the PPI network.

The ACACB protein, additionally termed ACC2, regulates fatty acid oxidation. It has been reported that *ACACB* may be involved in upregulated pathways, including the adipocytokine and type 2 diabetes signaling pathways (18). The knockout of *ACC2* has been demonstrated to exert a preventative effect on cardiac remodeling (19). In addition, the cardiac-specific deletion of *ACC2* in rats resulted in improved cardiac function (20). These previous results suggested that the upregulation of *ACC2* may be the primary cause of cardiac dysfunction. In the present study, associated with the carboxylic acid binding BP, ACC2 was identified to be an upregulated node in the PPI network of DEGs in AngII-induced cardiac remodeling, further supporting the causative role of ACC2 in cardiac remodeling. Additionally, ACC2 was significantly enriched in the carboxylic acid binding MF, suggesting it may regulate this function to exert its role in cardiac remodeling.

IL1B belongs to the interleukin 1 cytokine family. It is important for the regulation of inflammatory responses. Proinflammatory cytokines, including IL1B, are associated with cardiac dysfunction (21). The expression of transforming growth factor-β (*TGF-β*) is induced by AngII in primary human CFs, and it has been reported to downregulate a number of proinflammatory genes, including *IL1B* (22). This suggested that the expression of *IL1B* may be mediated by TGF-β. Conversely, the present study did not detect the gene

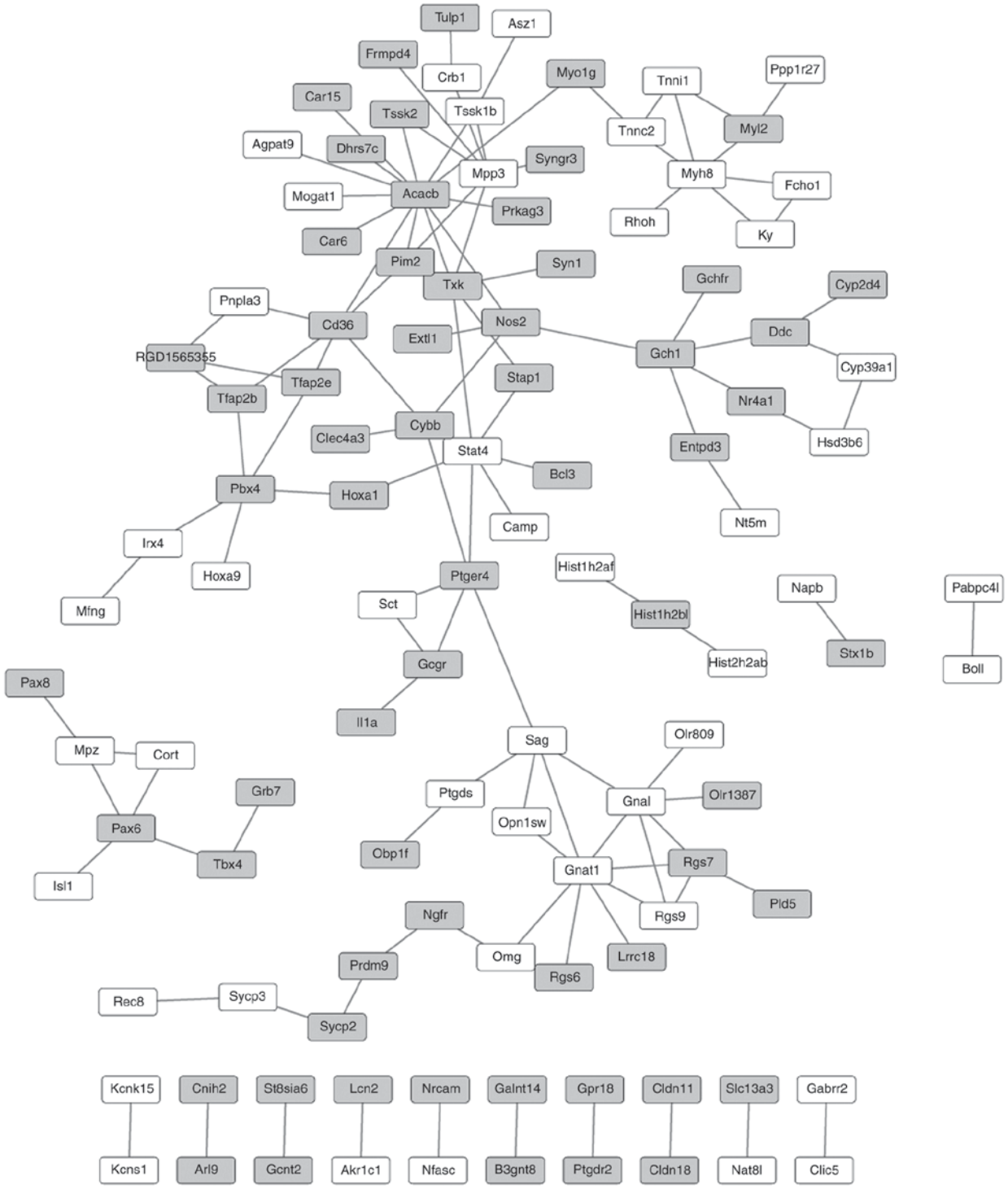

Figure 2. Protein-protein interaction network of differentially-expressed genes. Grey denotes upregulated genes and white denotes downregulated genes.

expression of *TGF-β*, although *IL1B* was upregulated, which was inconsistent with the previous study. It may be inferred that without the regulation of *TGF-β*, *IL1B* may be upregulated in cardiac remodeling. IL1A is another interleukin 1 cytokine family member that has important roles in the mediation of immune responses and hematopoiesis (23). Adverse cardiac remodeling results from an immune response driven by T helper 1 cells and type 1 macrophages (24). The results of the present study demonstrated that IL1A was significantly enriched in the immune response and regulation of angiogenesis BPs, suggesting that this gene may be important in AngII-induced cardiac remodeling via involvement in these above processes.

The *NOS2* gene may be induced by a number of cytokines in the liver. It has important roles in numerous processes, including antitumoral activities and the regulation of the defense response (25,26). Reportedly, suppression of NOS2 contributes to cardiac function recovery in rats by ameliorating cardiac remodeling (27). In a failing human heart, it has been demonstrated that NOS2 downregulates the

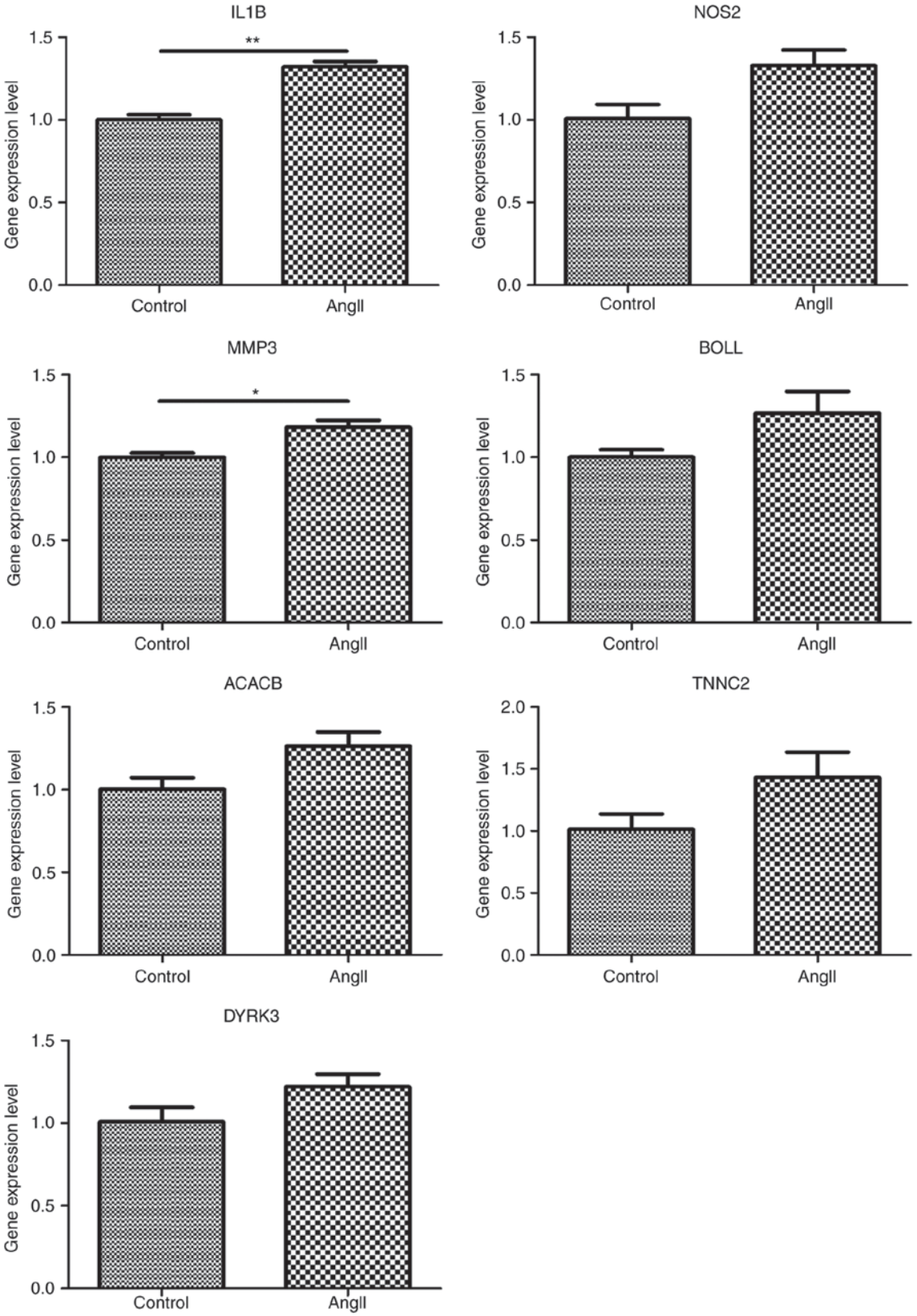

Figure 3. Validation of gene expression via reverse transcription-quantitative polymerase chain reaction. *P<0.05, **P<0.01. IL1B, interleukin 1β; NOS2, nitric oxide synthase 2; MMP3, matrix metallopeptidase 3; BOLL, boule homolog RNA binding protein; ACACB, acetyl coA carboxylase β; TNNC2, troponin C2 fast skeletal type; DYRK3, dual specificity tyrosine phosphorylation regulated kinase 3; AngII, angiotensin II.

muscular protein LIM/homeobox protein Lhx1, an important molecule for cardiac hypertrophy, thereby promoting adverse cardiac remodeling (28). In support of these previous findings, the results of the present study demonstrated that NOS2 was an upregulated gene that was enriched in the response to bacterium and defense response BPs, implying

it may be an important regulator in AngII-induced cardiac remodeling. Unfortunately, this upregulation was not validated by the RT-qPCR results, which may be due to the small sample size.

MMP3 is a membrane-associated protein. Increased expression of MMPs is frequently associated with cardiac remodeling (29). As a well-known target of osteopontin, MMP3 has been suggested to be a potential therapeutic target to inhibit cardiac remodeling, as its expression contributes to the progression of extensive fibrosis in acute myocarditis (30). In accordance with these previous results, the present study demonstrated that MMP3 was an upregulated gene in AngII-induced cardiac remodeling. Notably, MMP3 was highlighted in the PPI network, suggesting that it serve roles in the progression of AngII-induced cardiac remodeling by interacting with other genes.

The *AXL* encoded protein is a family member of the Tyro3-Axl-Mer (TAM) tyrosine receptors. Reportedly, the expression of *AXL* is a potential genetic marker for salt-dependent hypertension, and at early stage of this type of hypertension, *AXL* is associated with kidney pathology (31). In addition, in the hematopoietic compartment of early hypertensive kidneys, *AXL* mediates the expression of interferon γ (31) which controls the interactions between different macrophages and T cells in AngII-stimulated cardiac remodeling (32). The ablation of AXL may cause degenerative alterations to the hematopoietic system (33). Transplantation of cardiac resident stem cells (CRSCs) is considered to be a promising strategy for the treatment of heart disease. CRSCs have a cardioprotective effect and $W8B2^+$ CRSCs are reported to secrete cytokines that are potentially involved in cell growth and survival, including AXL (34). These previous results collectively indicated that increased expression of *AXL* may have a protective effect in cardiac remodeling, while decreased expression may cause or contribute to the progression of cardiac remodeling. Based on the RNA-seq results of the present study, although the expression of *AXL* was downregulated in AngII-treated CFs compared with the control, the difference was not significant. Further experiments are required to investigate the expression of *AXL* in AngII-induced cardiac remodeling.

Despite comprehensive analyses and validation experiments, a number of limitations remained in the present study. The sample size was small as each group contained only two samples. A gradient-concentration experiment to select the optimal AngII concentration was not performed, with the optimum concentration being inferred from a number of published articles. Although the expression of a number of genes was validated, their interactions as predicted in the PPI network were not validated. Therefore, further samples and concentration-response experiments are required in the future. However, the present study provided an insight into the AngII-induced cardiac remodeling mechanism and may facilitate the identification of potential therapeutic targets.

In conclusion, the dysregulation of 5 genes, *ACACB*, *IL1A*, *NOS2*, *IL1B* and *MMP3,* may be a primary cause of AngII-induced cardiac remodeling, and all of the genes, particularly *IL1B* and *MMP3,* may be used as candidate markers for prevention and treatment.

Acknowledgements

The present study was supported by the Changning District of Shanghai Science and Technology Commission (grant no. cnkw2014j03).

References

1. Takano H, Hasegawa H, Nagai T and Komuro I: Implication of cardiac remodeling in heart failure: Mechanisms and therapeutic strategies. Intern Med 42: 465-469, 2003.
2. Bujak M and Frangogiannis NG: The role of TGF-beta signaling in myocardial infarction and cardiac remodeling. Cardiovasc Res 74: 184-195, 2007.
3. Iwanaga K, Takano H, Ohtsuka M, Hasegawa H, Zou Y, Qin Y, Odaka K, Hiroshima K, Tadokoro H and Komuro I: Effects of G-CSF on cardiac remodeling after acute myocardial infarction in swine. Biochem Biophys Res Commun 325: 1353-1359, 2004.
4. Grobe JL, Mecca AP, Lingis M, Shenoy V, Bolton TA, Machado JM, Speth RC, Raizada MK and Katovich MJ: Prevention of angiotensin II-induced cardiac remodeling by angiotensin-(1-7). Am J Physiol Heart Circ Physiol 292: H736-H742, 2007.
5. Huang XR, Chung AC, Yang F, Yue W, Deng C, Lau CP, Tse HF and Lan HY: Smad3 mediates cardiac inflammation and fibrosis in angiotensin II-induced hypertensive cardiac remodeling. Hypertension 55: 1165-1171, 2010.
6. Hu C, Dandapat A, Sun L, Marwali MR, Inoue N, Sugawara F, Inoue K, Kawase Y, Jishage K, Suzuki H, *et al*: Modulation of angiotensin II-mediated hypertension and cardiac remodeling by lectin-like oxidized low-density lipoprotein receptor-1 deletion. Hypertension 52: 556-562, 2008.
7. McCalmon SA, Desjardins DM, Ahmad S, Davidoff KS, Snyder CM, Sato K, Ohashi K, Kielbasa OM, Mathew M, Ewen EP, *et al*: Modulation of angiotensin II-mediated cardiac remodeling by the MEF2A target gene Xirp2. Circ Res 106: 952-960, 2010.
8. Yang D, Yuan J, Liu G, Ling Z, Zeng H, Chen Y, Zhang Y, She Q and Zhou X: Angiotensin receptor blockers and statins could alleviate atrial fibrosis via regulating platelet-derived growth factor/Rac1/nuclear factor-kappa B Axis. Int J Med Sci 10: 812-824, 2013.
9. Chomczynski P and Sacchi N: The single-step method of RNA isolation by acid guanidinium thiocyanate-phenol-chloroform extraction: Twenty-something years on. Nat Protoc 1: 581-585, 2006.
10. Ran M, Chen B, Li Z, Wu M, Liu X, He C, Zhang S and Li Z: Systematic identification of long noncoding RNAs in immature and mature porcine testes. Biol Reprod 94: 77, 2016.
11. Pertea M, Pertea GM, Antonescu CM, Chang TC, Mendell JT and Salzberg SL: StringTie enables improved reconstruction of a transcriptome from RNA-seq reads. Nat Biotechnol 33: 290-295, 2015.
12. Huang DW, Sherman BT, Tan Q, Kir J, Liu D, Bryant D, Guo Y, Stephens R, Baseler MW, Lane HC and Lempicki RA: DAVID bioinformatics resources: Expanded annotation database and novel algorithms to better extract biology from large gene lists. Nucleic Acids Res 35 (Web Server Issue): W169-W175, 2007.
13. Szklarczyk D, Franceschini A, Kuhn M, Simonovic M, Roth A, Minguez P, Doerks T, Stark M, Muller J, Bork P, *et al*: The STRING database in 2011: Functional interaction networks of proteins, globally integrated and scored. Nucleic Acids Res 39 (Database Issue): D561-D568, 2011.
14. Livak KJ and Schmittgen TD: Analysis of Relative Gene Expression Data Using Real-Time Quantitative PCR and the 2(-Delta Delta C(T)) method. Methods 25: 402-408, 2001.
15. Santulli G: Sympathetic nervous system signaling in heart failure and cardiac aging. Pathophysiol Pharm Cardio Disease: 83-105, 2015.
16. Perrino C and Rockman HA: Reversal of cardiac remodeling by modulation of adrenergic receptors: A new frontier in heart failure. Curr Opin Cardiol 22: 443-449, 2007.
17. Karnik SS and Unal H: Angiotensin II receptor-induced cardiac remodeling in mice without angiotensin II. Hypertension 59: 542-544, 2012.

18. Ables GP, Ouattara A, Hampton TG, Cooke D, Perodin F, Augie I and Orentreich DS: Dietary methionine restriction in mice elicits an adaptive cardiovascular response to hyperhomocysteinemia. Sci Rep 5: 8886, 2015.
19. Hwang IW, Makishima Y, Kato T, Park S, Terzic A and Park EY: Human acetyl-CoA carboxylase 2 expressed in silkworm Bombyx mori exhibits posttranslational biotinylation and phosphorylation. Appl Microbiol Biotechnol 98: 8201-8209, 2014.
20. Yan H, Li Y, Wang C, Zhang Y, Liu C, Zhou K and Hua Y: Contrary microRNA expression pattern between fetal and adult cardiac remodeling: Therapeutic value for heart failure. Cardiovasc Toxicol 17: 267-276, 2017.
21. Salvador AM, Nevers T, Velázquez F, Aronovitz M, Wang B, Abadía Molina A, Jaffe IZ, Karas RH, Blanton RM and Alcaide P: Intercellular adhesion molecule 1 regulates left ventricular leukocyte infiltration, cardiac remodeling, and function in pressure overload-induced heart failure. J Am Heart Assoc 5: e003126, 2016.
22. Kapoun AM, Liang F, O'young G, Damm DL, Quon D, White RT, Munson K, Lam A, Schreiner GF and Protter AA: B-Type natriuretic peptide exerts broad functional opposition to transforming growth factor-beta in primary human cardiac fibroblasts, myofibroblast conversion, proliferation, and inflammation. Circ Res 94: 453-461, 2004.
23. Akula MK, Shi M, Jiang Z, Foster CE, Miao D, Li AS, Zhang X, Gavin RM, Forde SD, Germain G, *et al*: Control of the innate immune response by the mevalonate pathway. Nat Immunol 17: 922-929, 2016.
24. Bönner F, Borg N, Jacoby C, Temme S, Ding Z, Flögel U and Schrader J: Ecto-5'-nucleotidase on immune cells protects from adverse cardiac remodeling. Circ Res 113: 301-312, 2013.
25. Stych B: Regulation and role of RNA Pol II CTD phosphorylation in the transcription cycle of the Nos2 gene (unpublished PhD thesis). University of Vienna, 2014.
26. Sun J, Shi YH, Le GW and Ma XY: Distinct immune response induced by peptidoglycan derived from lactobacillus sp. World J Gastroenterol 11: 6330-6337, 2005.
27. Zheng B, Cao LS, Zeng QT, Wang X, Li DZ and Liao YH: Inhibition of NOS2 ameliorates cardiac remodeling, improves heart function after myocardial infarction in rats. Basic Res Cardiol 99: 264-271, 2004.
28. Kempf T and Wollert KC: Nitric oxide and the enigma of cardiac hypertrophy. Bioessays 26: 608-615, 2004.
29. Liao Y, Zhao H, Ogai A, Kato H, Asakura M, Kim J, Asanuma H, Minamino T, Takashima S and Kitakaze M: Atorvastatin slows the progression of cardiac remodeling in mice with pressure overload and inhibits epidermal growth factor receptor activation. Hypertens Res 31: 335-344, 2008.
30. Szalay G, Sauter M, Haberland M, Zuegel U, Steinmeyer A, Kandolf R and Klingel K: Osteopontin: A fibrosis-related marker molecule in cardiac remodeling of enterovirus myocarditis in the susceptible host. Circ Res 104: 851-859, 2009.
31. Batchu SN, Hughson A, Gerloff J, Fowell DJ and Korshunov VA: Role of Axl in early kidney inflammation and progression of salt-dependent hypertension. Hypertension 62: 302-309, 2013.
32. Han YL, Li YL, Jia LX, Cheng JZ, Qi YF, Zhang HJ and Du J: Reciprocal interaction between macrophages and T cells stimulates IFN-γ and MCP-1 production in Ang II-induced cardiac inflammation and fibrosis. PLoS One 7: e35506, 2012.
33. Arandjelovic S and Ravichandran KS: A MERry response after myocardial infarction. Circ Res 113: 949-951, 2013.
34. Zhang Y, Sivakumaran P, Newcomb AE, Hernandez D, Harris N, Khanabdali R, Liu GS, Kelly DJ, Pébay A, Hewitt AW, *et al*: Cardiac repair with a novel population of mesenchymal stem cells resident in the human heart. Stem Cells 33: 3100-3113, 2015.